Optical Materials 47 (2015) 478–483

Contents lists available at ScienceDirect

Optical Materials

journal homepage: www.elsevier.com/locate/optmat

Versatile liquid-core optofluidic waveguides fabricated in hydrophobic silica aerogels by femtosecond-laser ablation

Berna Yalizay [a], Yagiz Morova [a], Koray Dincer [a], Yaprak Ozbakir [b], Alexandr Jonas [a], Can Erkey [b], Alper Kiraz [c], Selcuk Akturk [a,*]

[a] Department of Physics, Istanbul Technical University, 34469 Maslak, Istanbul, Turkey
[b] Department of Chemical and Biological Engineering, Koç University, Rumelifeneri Yolu, 34450 Sariyer, Istanbul, Turkey
[c] Department of Physics, Koç University, Rumelifeneri Yolu, 34450 Sariyer, Istanbul, Turkey

ARTICLE INFO

Article history:
Received 27 March 2015
Received in revised form 20 May 2015
Accepted 10 June 2015
Available online 18 June 2015

Keywords:
Optofluidics
Light waveguides
Microfluidics
Aerogels
Femtosecond laser ablation

ABSTRACT

We report on the fabrication and characterization of versatile light waveguides exploiting filaments of a polar liquid confined within hydrophobic silica aerogels. Aerogels are highly porous materials with extremely low refractive index which makes them suitable as rigid cladding of liquid-core optofluidic waveguides based on total internal reflection of light. In this article, we introduce a new microfabrication technique that allows direct and precise processing of monolithic silica aerogels by ablation with femtosecond laser pulses. Using fast scanning of the focused laser ablation beam synchronized with the motion of the processed aerogel sample, we created high-quality straight microchannels of ~5 mm length with controlled cross-sections inside monolithic aerogels. After the ablation, we filled the channels with high-refractive index ethylene glycol, forming multimode liquid core – solid cladding optofluidic waveguides. Subsequently, we carried out light-guiding experiments to measure overall optical attenuation of these waveguides. The characterization of waveguide transmission yielded values of propagation losses lower than 10 dB cm^{-1}, demonstrating that the liquid-core waveguides with laser-ablated aerogel cladding represent an attractive alternative in optofluidic applications targeting controlled routing of light along arbitrary three-dimensional paths.

1. Introduction

Integrated optofluidic circuits that combine photonics with microfluidics have become increasingly popular experimental platforms for implementing novel optical devices and lab-on-a-chip analytical and preparative systems [1]. Optofluidic waveguides represent one of the basic building blocks of such circuits, serving as adjustable optical interconnects for routing the light from the source through the measurement or reaction compartment of the optofluidic system to the detector [2,3]. Besides allowing for direct integration of the fluidic and optical components within the same chip, optofluidic waveguides also enable efficient capture and delivery of light generated by molecules or small particles suspended in the working liquid and they can greatly increase the surface-to-volume ratio of the reaction part of the optofluidic chip. These properties are crucial for applications in light-driven processes including photometric and spectroscopic analysis of minute sample volumes and energy production based on the conversion of light energy in photosynthetic or photocatalytic reactions [4,5].

Optofluidic waveguides can be broadly classified into two main families: interference-based ones and total internal reflection (TIR)-based ones. Bragg fibers, hollow photonic crystal fibers and anti-resonant reflecting optical waveguides fall in the first category [6,7] while liquid core waveguides (LCWs) [8,9], slot waveguides [10], and liquid–liquid core waveguides [11] are prominent examples that fall in the second category. Among these alternatives, liquid core optofluidic waveguides represent the most straightforward way toward achieving light guiding. In this approach, a suitable solid material confines the core liquid within internal channels and, simultaneously, serves as the waveguide cladding. In order to enable propagation of non-lossy optical modes guided in the liquid by total internal reflection of light from the channel walls, the cladding material should have a low absorption coefficient at the working light wavelength and a refractive index smaller than that of the core liquid. In many applications – especially those involving biological samples – aqueous working liquids with refractive index ~1.33 are required. This poses an experimental challenge, as there

* Corresponding author.
E-mail address: selcuk.akturk@itu.edu.tr (S. Akturk).

http://dx.doi.org/10.1016/j.optmat.2015.06.024
0925-3467/

is only a limited choice of solid host materials available with the index of refraction below that of water.

To meet these refractive index requirements, thin coatings of amorphous Teflon-AF polymer deposited on glass, silicone, or polymer supporting substrates have been frequently employed [8,12–15]. Teflon-AF-based materials are optically transparent and have refractive index (RI) of 1.29–1.31, slightly lower than the refractive index of water. Various applications such as detectors, chemical sensors, and pollution measurement systems have been developed using LCWs with Teflon AF coatings [4,16–18]. However, Teflon AF has proven not to be an ideal material for many applications due to: (i) its poor adhesion to common solid substrates used for manufacturing of microfluidic chips, (ii) difficulties in chemical functionalization of the interface between Teflon AF coating and the aqueous core liquid, and (iii) low refractive index contrast which limits the fraction of photons generated within the aqueous core which can be efficiently collected and guided [9]. Lower refractive index materials such as nanoporous dielectrics [9] or silica aerogels [19,20] are therefore important cladding candidates for developing novel types and applications of LCWs.

Silica aerogels are highly porous nanostructured materials that can be synthesized as macroscopic monoliths with distinctive properties such as extremely low index of refraction and thermal conductivity, high surface area to volume ratio, and high optical transparency [21]. These properties, especially the very low RI of ~1.05, make aerogels a perfect solid-cladding material which does not require any additional coating, as almost all liquids have refractive indices exceeding the RI of silica aerogel. Moreover, aerogels can be chemically modified during synthesis in order to make them compatible with both polar and non-polar core liquids [21,22]. However, it is very challenging to machine aerogels using conventional mechanical processes such as cutting, drilling or milling because they are very fragile [23]. Therefore, there is a need to develop an alternative technique of forming optofluidic waveguides inside aerogel blocks without causing any damage to their monolithic structure. In recent studies, this issue was addressed by using a straight or U-shaped solid fiber which was embedded into the silica sol prior gelation and removed during or after the drying step [19,20]. The fiber embedded into the aerogel acted as a preform which left behind an empty channel after removal from the solid monolith. However, the preform-based methods provide only limited channel shaping and sizing capabilities.

In the last decade, multiple studies have shown that ultrafast laser machining can serve as a precise and easy method for processing a wide variety of materials including optical glasses, metals, polymers, and crystals with minimal mechanical and thermal damage [24]. When ultrafast laser pulses are employed for material ablation, thermal effects arising from the heat transfer between optically excited electrons and surrounding lattice are suppressed since the excitation light pulse ends well before the time scale needed for the thermal energy transfer is reached. Thus, heat diffusion outside of the beam focal area is minimized which leads to a very localized and clean ablation. Moreover, because of its strongly non-linear character, interaction between ultrafast light and material is confined to the high-intensity region in the immediate vicinity of the beam focus which further contributes to the high resolution and precision of the ultrafast laser micromachining [25]. Indeed, preliminary studies of ultrafast-light micromachining of silica aerogels have demonstrated that such aerogels can be precisely ablated with femtosecond lasers, thanks to their ultra-low thermal conductivity [26]. In the same study, it was also shown that sub-surface ablation is possible by focusing the ablation beam beneath the aerogel surface, even though the channels formed in this way are irregular due to beam phase distortions introduced by propagation through material of non-uniform thickness. However, laser-ablation-based generation of uniform channels in the bulk of monolithic aerogels has not been demonstrated previously.

In this work, we report on the formation of uniform, extended channels inside hydrophobic aerogel monoliths through femtosecond laser ablation and, subsequently, introduce TIR-based liquid-core optofluidic waveguides manufactured by direct femtosecond laser writing of such channels. Our waveguides use low-refractive index hydrophobic aerogels processed by laser ablation as the solid cladding and ethylene glycol filaments confined within the aerogels as the high-refractive index liquid cores. The combination of hydrophobic solid cladding with a polar core liquid ensures that the liquid remains confined within the channel and does not penetrate into the nanoporous structure of the aerogel monolith, thus maintaining the contrast of refractive index necessary for light guiding. We present an experimental procedure for manufacturing optofluidic waveguides of millimeter length. Subsequently, we characterize the light-guiding properties and propagation losses of our waveguides and show that they can serve for efficient light routing in integrated optofluidic systems.

2. Preparation of hydrophobic silica aerogel monoliths

Starting silica aerogels were synthesized using conventional two step sol–gel process [20,21,27,28]. We used tetraethylorthosilicate (TEOS) (98% purity; AlfaAesar) as a silica precursor, hydrochloric acid (HCl) (37% purity; Riedel-de Haen) as an acid catalyst, and ammonia (NH_3) (2.0 M in ethanol; Aldrich) as a base catalyst. Initially, we prepared the precursor solution by mixing TEOS, ethanol (99.9% purity; Merck) and water with a mass ratio of 1:1:0.34. To accelerate TEOS hydrolysis reactions, we added the acid catalyst (0.2 ml in 1 g TEOS: 1 g ethanol: 0.34 g water) and stirred the mixture at room temperature for 60 min. Subsequently, we added the base catalyst (0.5 ml in 1 g TEOS: 1 g ethanol: 0.34 g water) to the solution to increase the rate of silane condensation reactions. Before gelation, we transferred the solution into a cylindrical plastic mold (diameter = 2.8 cm; length = 2 cm) which was subsequently sealed. After gelation, we soaked the resulting alcogels in an aging solution (120 ml TEOS, 30 ml water, 150 ml ethanol) which was kept in an oven at 50 °C for 24 h. After one-day aging in the oven, we left the samples in the aging solution at room temperature for times varying between three and seven days. When the aging time is increased, additional silane monomers from the solution condense with already formed silane network. These additional condensation reactions then enhance the mechanical strength and stiffness of the alcogel. Finally, we washed the alcogels with fresh ethanol for 3 days in order to remove any impurities and water remaining in the pores of the alcogel. Subsequently, we dried the wet alcogels at 40 °C, 100 bar with supercritical CO_2 ($scCO_2$) in Applied Separations Speed SFE unit for 7 h. Following supercritical drying, we determined bulk density of each monolithic aerogel sample by dividing its mass with its volume. The density of the sample used in the optofluidic waveguide studies was 0.2 g/cm^3.

The index of refraction of porous silica aerogels can be calculated from the Clausius–Mossotti formula applied to a composite material with uniform distribution of individual components (in our case, solid silica and air) throughout the bulk of the material. Within this formalism, Wang et al. [29] determined the effective refractive index of silica aerogels as:

$$n - 1 = \frac{3}{2}\frac{\rho}{\rho_s}\frac{n_s^2 - 1}{n_s^2 + 2} \quad (1)$$

where n and n_s are the indices of refraction and ρ and ρ_s are the densities of the aerogel and silica, respectively. Using ρ_s = 2.2 g/cm^3, n_s = 1.457 (at 633 nm wavelength) and the aerogel density

mentioned above, we calculate that the index of refraction of our aerogels is $n = 1.037$.

In order to render the aerogels hydrophobic, dry silica aerogel monoliths were treated with hexamethyldisilazane (HMDS) vapor in a tightly sealed beaker. A stainless steel screen was placed in the middle of the beaker in order to prevent the contact between liquid HMDS and the aerogel. 10 mL of the liquid HMDS was put in the beaker while the aerogels were placed on top of the screen. The aerogels were subsequently exposed to HMDS vapor at 110 °C and ambient pressure for 5 h.

3. Femtosecond laser ablation

Fig. 1a shows an illustration of the experimental setup which was used for micromachining channels with defined cross-sections inside hydrophobic silica aerogel monoliths. The laser system adopted for the ablation experiments (s-Pulse; Amplitude Systemes) generated 550 fs pulses at the fundamental wavelength of 1030 nm with 1 kHz pulse repetition rate. At the laser output, a half-wave plate combined with a polarizer served to adjust the average laser output power. The samples were ablated with the maximum laser power of 180 mW at the specimen, corresponding to the pulse energy of 180 μJ. During ablation, the beam propagation direction was controlled with a dual-axis scanning galvo system (Thorlabs, GVS012) which was driven by a two-channel function generator. Subsequently, the beam was focused on the surface of a silica aerogel monolith through a scan lens (Thorlabs, LSM03-VIS) with a working distance of 25.9 mm. The diameter of the focused laser beam was estimated to be about 10 μm. To create an extended channel within the aerogel, the sample was moved along the optical axis of the system (z-direction) with a three-dimensional translation stage.

Microchannels with a desired cross-section were machined in two steps. Initially, sinusoidal signals with the same frequency (15 Hz) and amplitude and a phase difference of 90° were sent to both x- and y-axis of the galvo scanner, resulting in a circular motion of the ablation beam focus across the aerogel surface. This circular pattern defined the circumference of the channel cross-section. Subsequently, sinusoidal signals of identical amplitudes and different frequencies (15 Hz vs 16 Hz) were sent to the x- and y-axis of the beam scanner, obtaining a Lissajous pattern which swept the ablation beam focus across the inner part of the channel cross-section. Fig. 1b shows the overall two-step ablation pattern. Simultaneously with the x, y-motion of the beam focus provided by the galvo system, the sample was translated along the z-axis with a speed of 10 μm/s by the scanning stage. In this way, cylindrical microchannels with ~5 mm length and ~500–600 μm diameter could be reproducibly formed inside silica aerogel blocks.

4. Results and discussions

4.1. Characterization of ablated aerogel channels

Using direct femtosecond laser writing procedure described in detail in the Section 3, we were able to form high-quality microchannels inside hydrophobic silica aerogel monoliths. Fig. 2 presents scanning electron microscope (SEM) images of these aerogel microchannels. In Fig. 2a, input face of a typical channel is depicted, whereas Fig. 2b and c shows axial cross-sections of the channels. One of the most important factors that affect the maximal length of the channel that can be manufactured is the accumulation of ablated silica particles within the channel during sample processing. When the laser ablation is carried out close to the monolith surface, the ablated aerogel particles can escape into the surrounding atmosphere. However, when the ablation proceeds deeper into the aerogel piece, an increasing accumulation of silica particles inside the channel can be observed (see Fig. 2b). These particles cause scattering of the ablation laser beam and ultimately limit the maximal depth of the channel that can be produced. In order to prevent this phenomenon, we exposed the sample to a directed flow of high pressure (~4 atm) nitrogen gas during the ablation. Fig. 2c shows SEM image of the axial cross-section of a channel which was formed under nitrogen gas

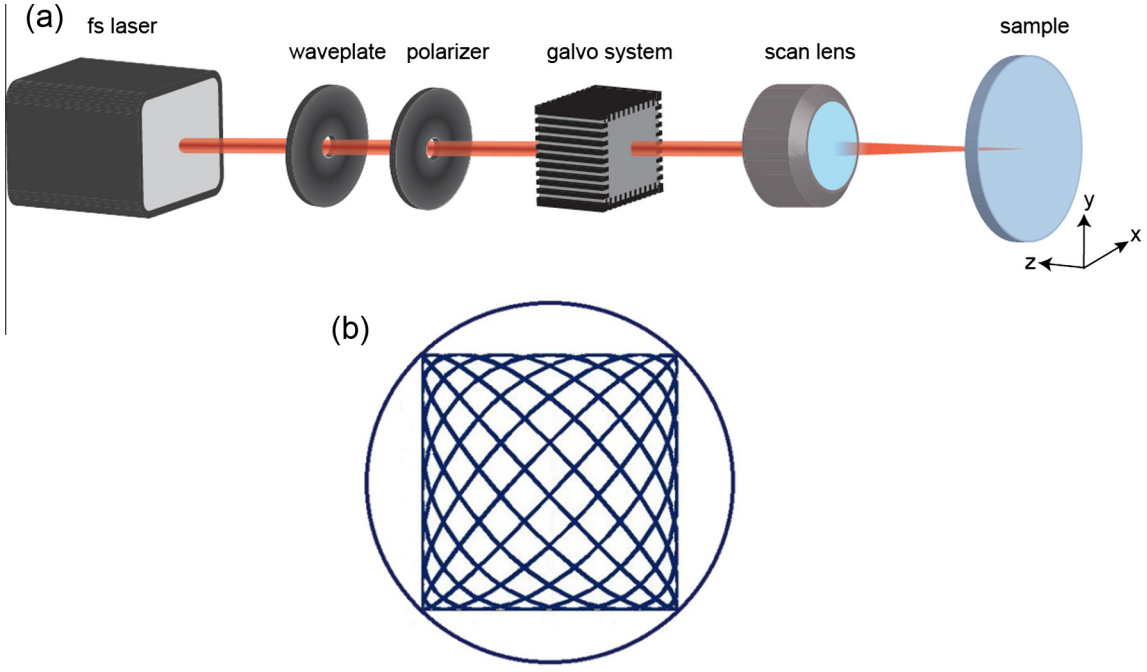

Fig. 1. (a) Illustration of the experimental setup used for aerogel micromachining by fs-laser ablation. (b) Detail of the xy-scanning pattern of the ablation beam over the aerogel surface.

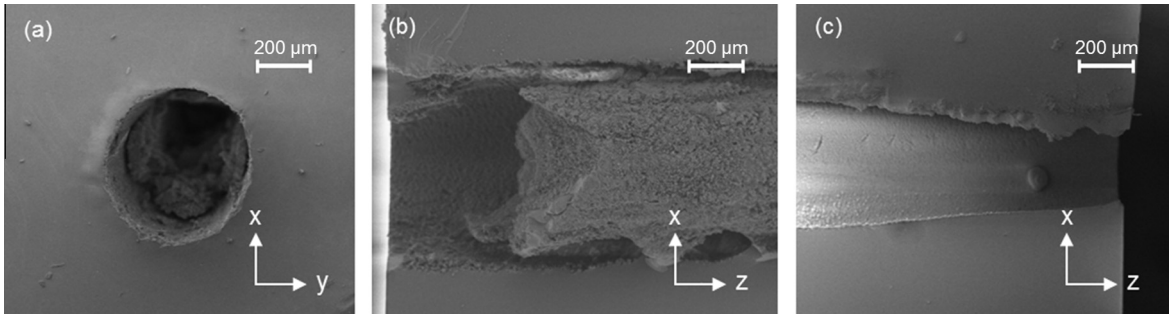

Fig. 2. SEM images of ablated aerogels. (a) Input face of a microchannel ablated inside the aerogel. The depth of the channel is about 300 μm and the diameter is about 500 μm. (b) Axial cross-section view of a channel ablated inside the aerogel. During machining, ablated silica particles accumulated inside the channel (see the right part of the channel). (c) Axial cross-section view of a channel ablated with simultaneous purging of the sample with high-pressure nitrogen gas. All the dust accumulated inside the channel during machining has been removed. For recording the cross-sectional images shown in (b) and (c), the samples were cleaved along the axis of the channel.

treatment. Comparison of Fig. 2b and c shows a clear improvement in the uniformity of the channel axial profile for nitrogen-treated samples, with all silica dust particles successfully removed by the nitrogen flow. Using this method, we succeeded in machining channels with the total length up to 5 mm. In order to improve further homogeneity of the fabricated channels, we scanned the ablation beam over the samples repeatedly up to four times.

4.2. Characterization of light-guiding properties of liquid-core optofluidic waveguides

After the successful formation of empty microchannels inside aerogel monoliths, we generated multimode optofluidic waveguides by filling the channels with a polar core liquid. Ultimately, our optofluidic waveguides are designed to operate with aqueous cores. However, relatively fast evaporation of water from open-ended channels created by laser ablation makes reliable quantitative measurements of the waveguide transmission losses challenging. For this reason, we chose to work with ethylene glycol in the waveguide characterization. This polar liquid has a significantly lower volatility than water and it is chemically compatible with the aerogel, i.e. it remains confined within the aerogel channels with hydrophobic walls and does not compromise the internal porous structure of aerogel monoliths. The calculation of the refractive index of silica aerogels (see Section 2) confirms that both ethylene glycol cores with the refractive index of 1.43 and aqueous cores with the refractive index of 1.33 lead to high-NA multimode optical waveguides: theoretical numerical aperture of the waveguide determined from the refractive indices of the liquid core and solid cladding as $\mathrm{NA} = \sqrt{n_{\mathrm{core}}^2 - n_{\mathrm{cladding}}^2}$ is 0.99 for ethylene glycol and 0.83 for water. The hydrophobicity of the channel walls makes the injection of the polar core liquid into the channel challenging. In order to fill the channels with the core liquid, we applied the following strategy. First, we blocked one end of the channel by placing the ablated aerogel monolith on a microscope slide. Subsequently, we slowly injected the liquid (with a syringe and a suitable thin tubing) from the open end of the channel. Slowly removing the cover plate then left the liquid inside the channel. To visualize the liquid confinement within the channel, we mixed ethylene glycol with fluorescein, an organic dye with peak excitation at 494 nm and peak emission at 521 nm. When illuminated with a blue laser light at 405 nm, sharply localized green fluorescence from the channel was clearly visible, as shown in Fig. 3 displaying photographs of the aerogel sample with an embedded liquid-core waveguide taken at two different magnifications. This verifies an excellent leak-free confinement of ethylene glycol within the channel which is a prerequisite for stable operation of the waveguide.

Fig. 4 illustrates experimental arrangement used for the characterization of light-guiding properties of our optofluidic waveguides

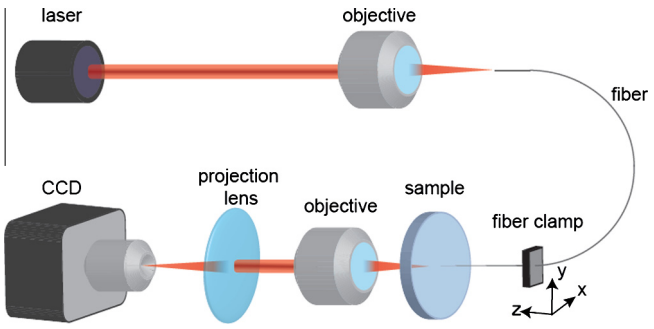

Fig. 4. Schematics of experimental setup used in the characterization of light-guiding performance of liquid core optofluidic waveguides.

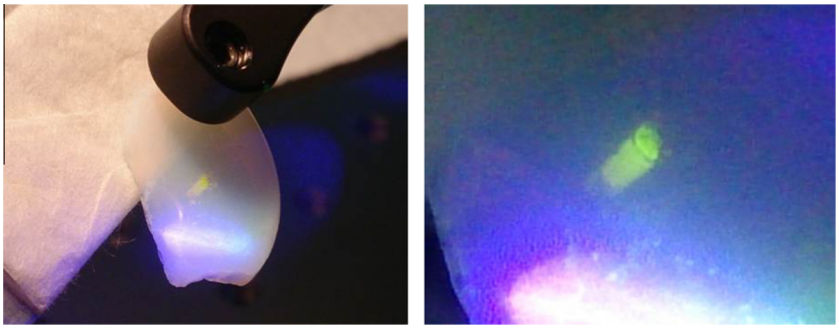

Fig. 3. Green fluorescence emitted from the aerogel channel filled with fluorescein-doped ethylene glycol solution upon illumination with blue light. (left) Overall picture of aerogel monolith with an embedded liquid-filled channel (right) detail of the liquid-filled channel. (For interpretation of the references to color in this figure legend, the reader is referred to the web version of this article.)

and measurement of their propagation losses. To this end, we coupled the light from an auxiliary diode laser (wavelength 632.8 nm) into the waveguide liquid core through a tapered optical fiber with an effective output numerical aperture (NA) of 0.57 and taper end diameter ~5 μm. High NA of the input fiber leads to a wider divergence angle of the light coupled into the waveguide. Consequently, the light requires a shorter propagation distance along the waveguide axis to reach the channel walls from which it is totally internally reflected. This increases the length of the channel which can be used to effectively guide the input light. To quantify the amount of light transmitted through the waveguide, we imaged the exit face of the liquid-filled channel on a CCD camera (Thorlabs DCU223M) using a microscope objective (Olympus RMS4x) in combination with a projection lens. With the diameter of the channel being 600 μm and the output NA of the coupling fiber being approximately 0.57, the beam diverging from the end of the tapered fiber centered on the channel axis reaches the walls of the channel after propagating approximately 1.1 mm along the channel axis. After this distance, the light fulfilling the TIR conditions reflects off the channel walls and propagates confined inside the channel.

In order to measure the propagation losses of the waveguide, we moved the coupling fiber along the channel axis and, simultaneously, monitored the total power of the light exiting the channel. This was achieved by summing the grayscale values of all pixels in the image of the waveguide exit face. An illustration image of the guided laser light can be seen in Fig. 5. Recorded light distribution covering the entire channel cross-section indicates that the coupled light was confined and guided inside the channel. Because of the multimode behavior of our large-core waveguides, the output light distribution features a characteristic speckle pattern arising from interference of individual guided modes.

We recorded the images of the output intensity distribution for 100 μm increments of the input fiber position along the channel axis. Subsequently, we plotted the total transmitted power (intensity integrated over the channel cross-section) as a function of the propagation distance along the waveguide. The results of a typical series of measurements are shown in Fig. 6. As illustrated in this figure, the measured output power of the waveguide displays regular oscillations superimposed on an exponentially decreasing background. These oscillations can be attributed to beating of multiple guided modes that propagate in the channel and whose relative phases change as the input fiber is translated along the waveguide axis. Mode beating was also observed in an alternative transmission measurement scheme in which the input tapered optical fiber was kept fixed and the transmitted light was collected by a single-mode probe fiber (8 μm core, 125 μm cladding diameter) inserted into the channel from the output end. Light coupled into the probe fiber was then detected by a photomultiplier tube for varying positions of the probe fiber along the channel axis. Measured photocurrent values exhibited oscillations with about the same periodicity as that obtained with the CCD method.

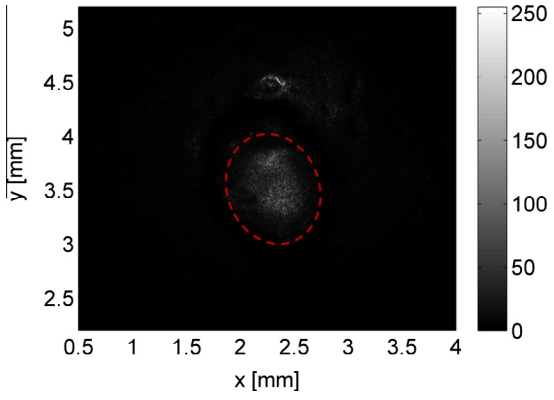

Fig. 5. Grayscale CCD image of guided light in the liquid-core waveguide embedded inside the aerogel. Red dashed curve indicates the channel contour and the light outside the region delimited by the curve result from scattering losses. (For interpretation of the references to color in this figure legend, the reader is referred to the web version of this article.)

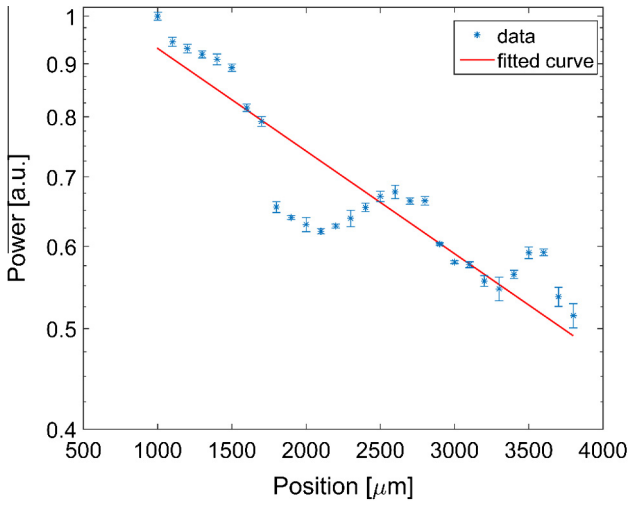

Fig. 6. Normalized power of light transmitted through the waveguide versus the propagation distance along the waveguide axis, shown in semi-log scale.

In order to quantify the propagation losses of the waveguide, we fitted the experimental values of the transmitted light power obtained from CCD measurements with an exponential curve of the form $P(z) = P_o \exp(-\alpha z)$ where z is the propagation distance along the waveguide axis. For the particular data set shown in Fig. 6, the obtained value of $\alpha = 2.278\ \mathrm{cm}^{-1}$. Hence, the propagation loss of the waveguide in the units of dB/cm can be calculated from

$$\eta = -\frac{10\alpha}{\ln 10} \tag{2}$$

According to Eq. (2), $\eta = -9.9$ dB/cm. This value is comparable to the propagation losses measured previously for alternative liquid-core optofluidic waveguide platforms [13,30].

5. Conclusions

In conclusion, we have demonstrated fabrication of multimode liquid-core optofluidic waveguides based on empty channels created inside hydrophobic silica aerogels by femtosecond laser micromachining and subsequently filled with ethylene glycol. We have investigated light-guiding properties of thus manufactured waveguides and measured their optical propagation losses. The experimentally obtained light-guiding characteristics show the potential of aerogel-based waveguides for efficient routing of light in optofluidic lightwave circuits. Due to strong confinement of the ablation process to the focal volume of the ablation laser beam, sub-micrometer-sized structures can be in principle generated [31]. Even though we have studied straight optofluidic waveguides in the present work, femtosecond ablation enables fabrication of arbitrary three-dimensional paths within the translucent silica aerogels, thus expanding significantly the application range of aerogel-based optofluidics. Experiments with manufacturing curved liquid-core optofluidic waveguides and additional elements of photonic circuits (e.g. Y-junctions) are currently underway. In a

practical optofluidic system based on the proposed waveguides, working liquid will be contained in a closed network of channels which are not exposed to the ambient atmosphere. Therefore, evaporation of the core liquid will not be an issue and ethylene glycol can be replaced with water without sacrificing waveguiding performance. Thus, our waveguides can also be utilized in experiments with live cells maintained in their natural aqueous environments for prolonged times.

Acknowledgements

This work was partially supported by the Scientific and Technological Research Council of Turkey (TÜBİTAK, Grant No. 112T972).

References

[1] Y. Fainman, L. Lee, D. Psaltis, C. Yang, Optofluidics: Fundamentals, Devices, and Applications, first ed., McGraw-Hill Professional, New York, 2009.
[2] H. Schmidt, A.R. Hawkins, Optofluidic waveguides: I. concepts and implementations, Microfluidics Nanofluidics 4 (2008) 3–16.
[3] A.R. Hawkins, H. Schmidt, Optofluidic waveguides: II. Fabrication and structures, Microfluidics Nanofluidics 4 (2008) 17–32, http://dx.doi.org/10.1007/s10404-007-0194-z.
[4] T. Dallas, P.K. Dasgupta, Light at the end of the tunnel: recent analytical applications of liquid-core waveguides, TrAC Trends Anal. Chem. 23 (2004) 385–392, http://dx.doi.org/10.1016/S0165-9936(04)00522-9.
[5] D. Erickson, D. Sinton, D. Psaltis, Optofluidics for energy applications, Nat. Photonics 5 (2011) 583–590, http://dx.doi.org/10.1038/nphoton.2011.209.
[6] A.M. Cubillas, S. Unterkofler, T.G. Euser, B.J.M. Etzold, A.C. Jones, P.J. Sadler, et al., Photonic crystal fibres for chemical sensing and photochemistry, Chem. Soc. Rev. 42 (2013) 8629, http://dx.doi.org/10.1039/c3cs60128e.
[7] R. Bernini, S. Campopiano, L. Zeni, P.M. Sarro, ARROW optical waveguides based sensors, Sens. Actuators B Chem. 100 (2004) 143–146, http://dx.doi.org/10.1016/j.snb.2003.12.035.
[8] R. Altkorn, I. Koev, A. Gottlieb, Waveguide capillary cell for low-refractive-index liquids, Appl. Spectrosc. 51 (1997) 1554–1558.
[9] W. Risk, H. Kim, R. Miller, H. Temkin, S. Gangopadhyay, Optical waveguides with an aqueous core and a low-index nanoporous cladding, Opt. Express. 12 (2004) 6446–6455, http://dx.doi.org/10.1364/OPEX.12.006446.
[10] Q. Xu, V.R. Almeida, R.R. Panepucci, M. Lipson, Experimental demonstration of guiding and confining light in nanometer-size low-refractive-index material, Opt. Lett. 29 (2004) 1626, http://dx.doi.org/10.1364/OL.29.001626.
[11] D.B. Wolfe, R.S. Conroy, P. Garstecki, B.T. Mayers, M.A. Fischbach, K.E. Paul, et al., Dynamic control of liquid-core/liquid-cladding optical waveguides, Proc. Natl. Acad. Sci. U. S. A. 101 (2004) 12434–12438, http://dx.doi.org/10.1073/pnas.0404423101.
[12] S.H. Cho, J. Godin, Y.-H. Lo, Optofluidic waveguides in Teflon AF-coated PDMS microfluidic channels, IEEE Photonics Technol. Lett. 21 (2009) 1057–1059, http://dx.doi.org/10.1109/LPT.2009.2022276.
[13] R. Manor, A. Datta, I. Ahmad, M. Holtz, S. Gangopadhyay, T. Dallas, Microfabrication and characterization of liquid core waveguide glass channels coated with Teflon AF, IEEE Sens. J. 3 (2003) 687–692, http://dx.doi.org/10.1109/JSEN.2003.820342.
[14] A. Datta, I.-Y. Eom, A. Dhar, P. Kuban, R. Manor, I. Ahmad, et al., Microfabrication and characterization of Teflon AF-coated liquid core waveguide channels in silicon, IEEE Sens. J. 3 (2003) 788–795, http://dx.doi.org/10.1109/JSEN.2003.820343.
[15] C.-W. Wu, G.-C. Gong, Fabrication of PDMS-based nitrite sensors using Teflon AF coating microchannels, IEEE Sens. J. 8 (2008) 465–469, http://dx.doi.org/10.1109/JSEN.2008.918201.
[16] C. Gooijer, G.P. Hoornweg, T. de Beer, A. Bader, D.J. van Iperen, U.A.T. Brinkman, Detector cell based on plastic liquid-core waveguides suitable for aqueous solutions: one-to-two decades improved detection limits in conventional-size column liquid chromatography with absorption detection, J. Chromatogr. A 824 (1998) 1–5, http://dx.doi.org/10.1016/S0021-9673(98)00668-2.
[17] P. Dress, M. Belz, K.F. Klein, K.T.V. Grattan, H. Franke, Water-core waveguide for pollution measurements in the deep ultraviolet, Appl. Opt. 37 (1998) 4991–4997, http://dx.doi.org/10.1364/AO.37.004991.
[18] B. Schelle, P. Dreß, H. Franke, K.F. Klein, J. Slupek, Physical characterization of lightguide capillary cells, J. Phys. Appl. Phys. 32 (1999) 3157, http://dx.doi.org/10.1088/0022-3727/32/24/311.
[19] L. Xiao, T.A. Birks, Optofluidic microchannels in aerogel, Opt. Lett. 36 (2011) 3275–3277.
[20] G. Eris, D. Sanli, Z. Ulker, S.E. Bozbag, A. Jonás, A. Kiraz, et al., Three-dimensional optofluidic waveguides in hydrophobic silica aerogels via supercritical fluid processing, J. Supercrit. Fluids 73 (2013) 28–33, http://dx.doi.org/10.1016/j.supflu.2012.11.001.
[21] A. Soleimani Dorcheh, M.H. Abbasi, Silica aerogel; synthesis, properties and characterization, J. Mater. Process. Technol. 199 (2008) 10–26, http://dx.doi.org/10.1016/j.jmatprotec.2007.10.060.
[22] A. Du, B. Zhou, Z. Zhang, J. Shen, A special material or a new state of matter: a review and reconsideration of the aerogel, Materials 6 (2013) 941–968, http://dx.doi.org/10.3390/ma6030941.
[23] K.E. Parmenter, F. Milstein, Mechanical properties of silica aerogels, J. Non-Cryst. Solids 223 (1998) 179–189, http://dx.doi.org/10.1016/S0022-3093(97)00430-4.
[24] R.R. Gattass, E. Mazur, Femtosecond laser micromachining in transparent materials, Nat. Photonics 2 (2008) 219–225, http://dx.doi.org/10.1038/nphoton.2008.47.
[25] F. He, Y. Liao, J. Lin, J. Song, L. Qiao, Y. Cheng, et al., Femtosecond laser fabrication of monolithically integrated microfluidic sensors in glass, Sensors 14 (2014) 19402–19440, http://dx.doi.org/10.3390/s141019402.
[26] J. Sun, J.P. Longtin, P.M. Norris, Ultrafast laser micromachining of silica aerogels, J. Non-Cryst. Solids 281 (2001) 39–47, http://dx.doi.org/10.1016/S0022-3093(00)00426-9.
[27] S. Gutzov, N. Danchova, S.I. Karakashev, M. Khristov, J. Ivanova, J. Ulbikas, Preparation and thermal properties of chemically prepared nanoporous silica aerogels, J. Sol–Gel Sci. Technol. 70 (2014) 511–516, http://dx.doi.org/10.1007/s10971-014-3315-7.
[28] J.L. Gurav, I.-K. Jung, H.-H. Park, E.S. Kang, D.Y. Nadargi, Silica aerogel: synthesis and applications, J. Nanomater. 2010 (2010) e409310, http://dx.doi.org/10.1155/2010/409310.
[29] P. Wang, A. Beck, W. Korner, H. Scheller, J. Fricke, Density and refractive index of silica aerogels after low- and high-temperature supercritical drying and thermal treatment, J. Phys. Appl. Phys. 27 (1994) 414, http://dx.doi.org/10.1088/0022-3727/27/2/036.
[30] A. Jonáš, B. Yalizay, S. Akturk, A. Kiraz, Free-standing optofluidic waveguides formed on patterned superhydrophobic surfaces, Appl. Phys. Lett. 104 (2014) 091123, http://dx.doi.org/10.1063/1.4867887.
[31] A.P. Joglekar, H. Liu, E. Meyhöfer, G. Mourou, A.J. Hunt, Optics at critical intensity: applications to nanomorphing, Proc. Natl. Acad. Sci. U. S. A. 101 (2004) 5856–5861, http://dx.doi.org/10.1073/pnas.0307470101.